

## Supplementary Information:

### Methods

#### A. Quantification of the extent of co-localization between CIC-7 and fluorescent fA $\beta$ -labeled lysosomes (relative co-localization index).

To quantify the relative co-localization index between CIC-7 and the fA $\beta$ -labeled lysosomes, we measured the ratio—

$$\frac{\text{CIC-7 fluorescence in the lysosomes}}{\text{Total CIC-7 fluorescence inside the cell}}$$

The image analysis was performed on maximum intensity projection images that were generated from confocal stacks. Image processing was done using MetaMorph image processing software (Universal Imaging, Molecular Devices, Sunnyvale, CA).

The image shown in Figure S8Ba shows a typical maximum projection image of CIC-7 staining that consists of two types of fluorescent objects: (i) large peri-nuclear structures and (ii) small punctate structures (indicated by white arrow). To quantify the fraction of CIC-7 in the punctate structures that co-localize with the fA $\beta$  positive lysosomes, we generated an image for the CIC-7 staining that only consisted of the punctate structures and excluded the large peri-nuclear aggregates.

For that purpose, we first used thresholding and morphometry analysis to generate a binary mask (Mask I) from the CIC-7 image that only consisted of the large peri-nuclear structures (Figure S8Bb). We eliminated fluorescence under Mask-I from the CIC-7 maximum projection image to yield a CIC-7 image that consisted only of the punctate structures in the cell periphery. We then applied a threshold to the fA $\beta$  image to identify the fA $\beta$ -labeled lysosomes and identified regions that included the thresholded objects. We transferred those regions to the modified CIC-7 image and measured the total fluorescence power in those regions, which corresponded to the CIC-7 fluorescence in the lysosomes. To quantify the total CIC-7 fluorescence inside the cells we used a low threshold and created a binary mask (Mask II) that included the entire CIC-7 signal inside each cell (Figure S8Bc). We then quantified the total fluorescence power in those regions to obtain the total CIC-7 signal inside the cell. For each experimental set, relative co-localization index was measured from at least 20 different cells.

## **B. Analysis of CIC-7 and LAMP1 localization in CD11b positive microglial cells in brain slices from the Tg19959 mouse.**

Free floating tissue sections from Tg19959 mice harboring human APP<sub>695</sub> with KM670/671NL and V717F mutations were immunostained with antibodies against CIC-7 or LAMP1 along with antibodies against CD11b for 24 hrs. After the 24 hrs, the tissue sections were incubated with appropriate fluorescently labeled secondary antibodies, and were imaged by confocal microscopy. For image acquisition, the microglial cells were selected based on their CD11b cell surface staining, and stacks of confocal images corresponding to the entire cell volume were collected. The images were acquired at relatively high magnification so that individual microglia were easily identifiable by the CD11b stain. Figure S11 (B,D) shows representative images of the CIC-7 and LAMP 1 staining in these cells. To compare the localization of CIC-7 and LAMP1 in microglial cells in these tissue sections, blinded investigators were asked to generate 3-dimensional outlines of the cells based on the CD11b staining. Image stacks corresponding to CIC-7 and LAMP-1 staining exclusively within the microglial cell boundary were then generated. Sum projection images were made from these confocal stacks, and Figure S11 (C, E) shows representative sum projection images that were made after applying the binary masks to CIC-7 and LAMP1 images. The sum projection images were provided to blinded investigators, and they were asked to bin the microglial cells based on the diffuse or punctate staining pattern. Cells that were most punctuate were scored as (+) 2 type cells (Figure 7I), while those with mostly diffuse staining were scored as (-) 2 type cells (Figure 7E). Cells with a mixed pattern were given intermediate scores. Scores were assigned for 30 cells from 30 different image stacks.

### **Supplementary Figure Legends:**

#### **Figure S1: Localization of CIC-7 in U2OS-SRA and J774 cells.**

(A-C) Immunolocalization of CIC-7 (green) as compared to Cy3fA $\beta$  (red) that had been endocytosed and delivered to lysosomes in U2OS-SRA cells. (D-F) Immunolocalization of CIC-7 (green) as compared to Cy3fA $\beta$  (red) that had been endocytosed and delivered to lysosomes in J774 macrophages.

(G-I) Immunolocalization of LAMP1 (green) as compared to Cy3fA $\beta$  (red) that had been endocytosed and delivered to lysosomes in primary mouse microglial cells. The images are single slices from a confocal stack. Bars: 5  $\mu$ m.

**Figure S2: Co-localization of CIC-7 with lysosomal, ER and Golgi markers in primary mouse microglial cells.**

(A-C) Immunolocalization of CIC-7 (green) and LAMP1 (red).

(D-F) Immunolocalization of CIC-7 (red) and a Golgi enzyme, Mannosidase II (green).

(G-I) Immunolocalization of CIC-7 (green) and an ER protein, Protein Disulphide Isomerase (red). The images are single slices from a confocal stack. Bars: 5  $\mu$ m.

**Figure S3: CIC-7 in primary mouse microglia forms peri-nuclear deposits that require microtubules and co-localize with poly-ubiquitinated proteins.**

(A-C) CIC-7 (green) immunolocalization in DMSO treated primary microglial cells.

Hoechst 33258 (blue) dye is used for staining nuclei. (D-F) CIC-7 (green) immunolocalization in nocodazole treated primary microglia.

(G) Detergent solubility of CIC-7. Microglial cells were lysed with buffer containing 1% Triton-X-100 following protocols described in the methods section. After cell lysis the lysate was separated into supernatant (S) and pellet (P) fractions and was analyzed by SDS-PAGE, followed by immunoblotting with antibody against CIC-7. GAPDH was used as a marker for the soluble supernatant.

**Figure S4. Localization of poly-ubiquitinated proteins and CIC-7 in primary mouse microglia.**

(A-C) Immunolocalization of CIC-7 (green) and poly-ubiquitinated proteins (red). The images are single slices from a confocal stack. Bars: 5  $\mu$ m.

**Figure S5: Determination of counterion permeability in the lysosomes of microglia.**

Determination of counterion permeability in the lysosomes of microglia with and without MCSF treatment II. The protonophore CCCP was used to rapidly dissipate the pH gradient in the presence of bafilomycin A1, and the lysosomal pH was monitored as a

function of time using protocols described in the methods section. For each data point about 50 vesicles from a single field were imaged, and four such fields were tracked simultaneously. The vacuolar H<sup>+</sup>-ATPase was inhibited with 0.4 μM Bafilomycin A1, and 20 μM CCCP was used. Addition of 50mM methylamine chloride was used to dissipate the pH gradient.

**Figure S6: Knockdown of CIC-7 expression in primary mouse microglia by siRNA.**

(A) Expression of CIC-7 protein detected by immunoblot. Lane (i) CIC-7 siRNA transfected set, lane (ii) non-target control siRNA transfected set.

(B) Expression of CIC-7 mRNA detected by RT-PCR. Lanes (i) and (iii) CIC-7 mRNA in the CIC-7 siRNA transfected and the control, non-target siRNA transfected sets, respectively. Lanes (ii) and (iv) GAPDH mRNA in the CIC-7 siRNA and non-target siRNA transfected sets, respectively.

(C) Knockdown of CIC-7 protein detected by immunofluorescence using an anti-CIC-7 polyclonal antibody. (i) Control, non-target siRNA transfected cells. (ii) CIC-7 siRNA transfected cells. Bars: 5 μm.

**Figure S7: Degradation of Cy3fAβ by MCSF-treated microglia after CIC-7 knockdown.**

(A) Degradation of Cy3fAβ by MCSF I treated primary microglia after control and CIC-7 siRNA transfection. Cy3 fluorescence retained inside the cells 72 hrs after a one hour uptake of Cy3fAβ is shown. Error bars represent S.E.M., and P values are obtained using Student's t test (two tailed).

(B). Knockdown of CIC-7 protein in microglia detected by immunofluorescence. The integrated fluorescence power per cell normalized to the fluorescence signal obtained after control siRNA transfection is shown. Error bars represent S.E.M., and P values are obtained using Student's t test (two tailed).

**Figure S8: Expression of Ostm1 protein in J774 macrophages, U2OS-SRA cells, and primary mouse microglia.**

(A) Ostm1 protein expression in total cell lysates from J774 macrophages, U2OS-SRA cells and primary mouse microglia. \* indicates the position of non-specific bands. Total protein loaded in each lane is 12  $\mu$ g.

(B) (a) Maximum intensity projection image of CIC-7 immunolocalization in primary mouse microglia. (b) Binary mask generated from the CIC-7 maximum intensity projection image that only consists of peri-nuclear CIC-7 structures. (c) Binary mask generated from the CIC-7 maximum intensity projection image that consists of total CIC-7 fluorescence inside the cells.

(C) Immunolocalization of V5 tagged Ostm1 (green) as compared to Cy3fA $\beta$  (red) that had been endocytosed and delivered to lysosomes in primary microglia after V5-Ostm1 over-expression. The image is a single slice from a confocal stack. Bar: 5  $\mu$ m.

(D) As a control for effects of transfection, primary microglial cells were transfected with Ds-Red (red), and the distribution of CIC-7 (green) was determined by immunolocalization. The outlines of the three cells in the field are shown in the merged image. The image is a single slice from a confocal stack. Bar: 5  $\mu$ m.

**Figure S9: Knockdown of Ostm1 in primary mouse microglia by siRNA.**

(A) Knockdown of Ostm1 mRNA detected by RT-PCR. Lanes (i) and (iii) Ostm1 mRNA in the control, non-target siRNA transfected and the Ostm1 siRNA transfected sets, respectively. Lanes (ii) and (iv) GAPDH mRNA in the control, non-target siRNA transfected and the Ostm1 siRNA transfected sets, respectively.

(B) Knockdown of Ostm1 protein detected by Western blot. Lane (i) Non-target control siRNA transfected set, lane (ii) Ostm1 siRNA transfected set.

**Figure S10: Degradation of Cy3fA $\beta$  by MCSF treated microglia after Ostm1 knockdown.**

(A) Degradation of Cy3fA $\beta$  by MCSF I treated primary microglia after control and Ostm1 siRNA transfection. Cy3 fluorescence retained inside the cells 72 hrs after a one hour uptake of Cy3fA $\beta$  is shown. Error bars represent S.E.M., and P values are obtained using Student's t test (two tailed).

(B) Knockdown of Ostm1 protein after siRNA transfection detected by Western blot. Lane (i) Ostm1siRNA3 transfected set, lane (ii) Control siRNA transfected set (iii) Ostm1 siRNA2 transfected (iv) Control siRNA transfected set.

(C). Knockdown of Ostm1 mRNA in primary mouse microglia after siRNA transfection. Data represents relative levels of Ostm1 mRNA after siRNA3 or siRNA2 transfection as compared to control siRNA-transfected microglia. The fold change in the mRNA levels were obtained from qRT-PCR experiments and calculated by the  $\Delta\Delta C_T$  method. Error bars represent S.E.M

**Figure S11: CIC-7 staining in brain slices from Tg19959 mice.**

(A) Immunolocalization of CIC-7 (green) in CA1 region neurons of a Tg19959 mouse. The images are single slices from a confocal stack. Bar: 25  $\mu\text{m}$ .

(B) Immunolocalization of CIC-7 (green) in CD11b positive microglial cells (red). The images are single slices from a confocal stack. Bar: 10  $\mu\text{m}$ .

(C) Sum projection image of a microglial cell generated from the image in panel B after the application of a binary mask consisting only of cell area covered by CD11b-labeled microglial cell.

(D) Immunolocalization of LAMP1 (green) in CD11b-labeled microglial cells (red). The images are single slices from a confocal stack. Bar: 7.5  $\mu\text{m}$ .

(E) Sum projection image of a microglial cell generated from the image in panel D after the application of a binary mask consisting only of cell area covered by CD11b-labeled microglial cell.

Figure S1

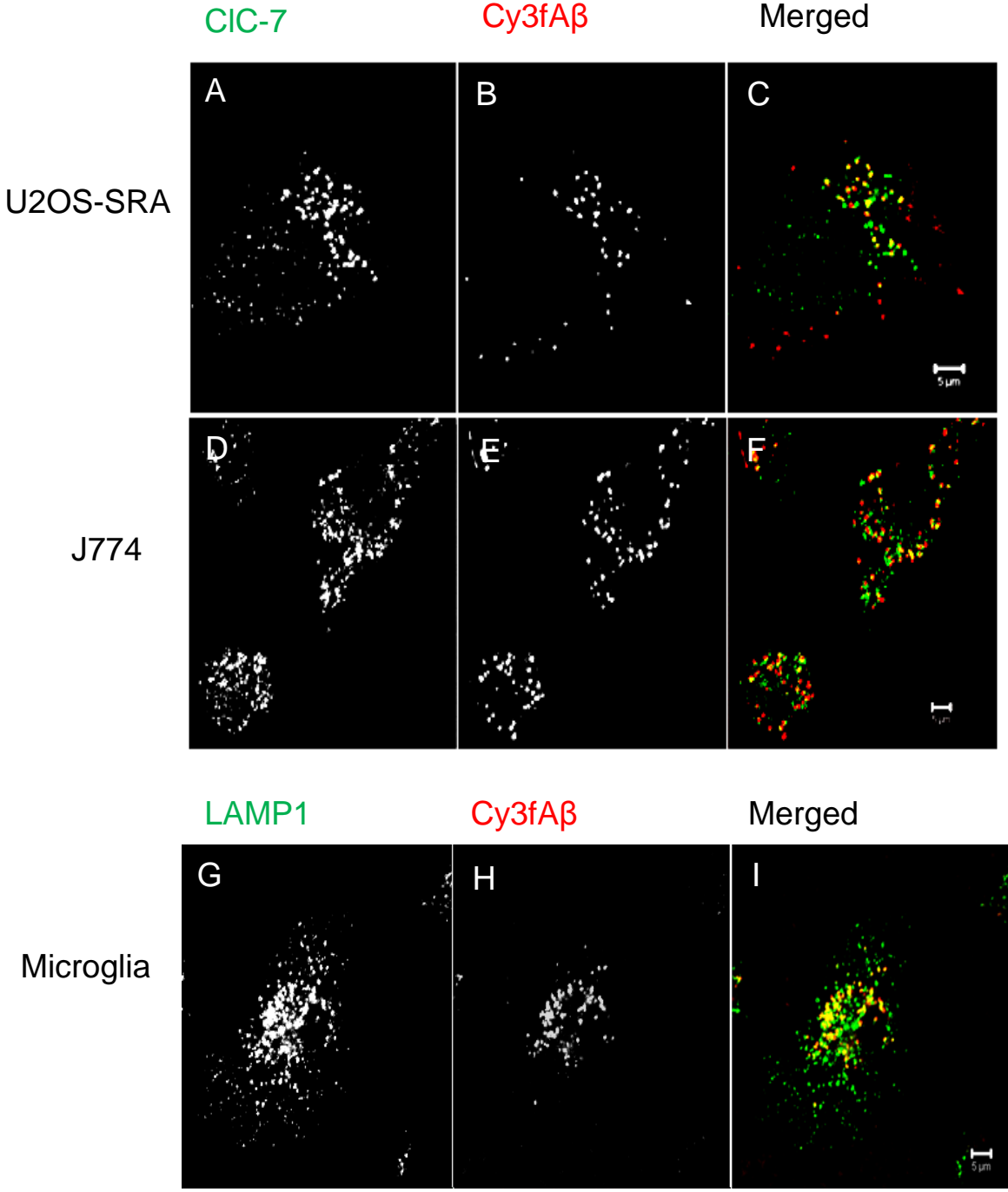


**Figure S2**

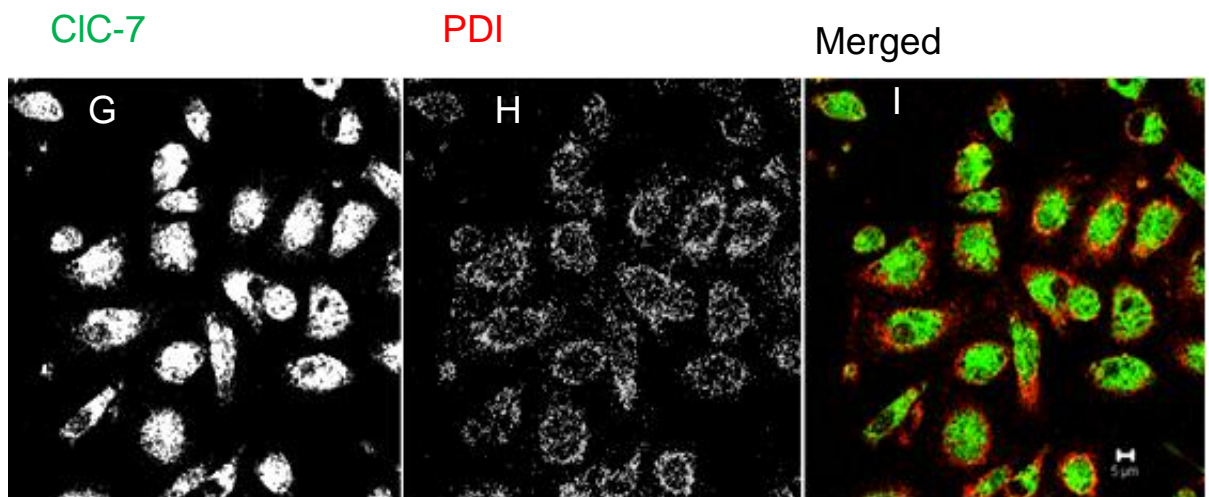
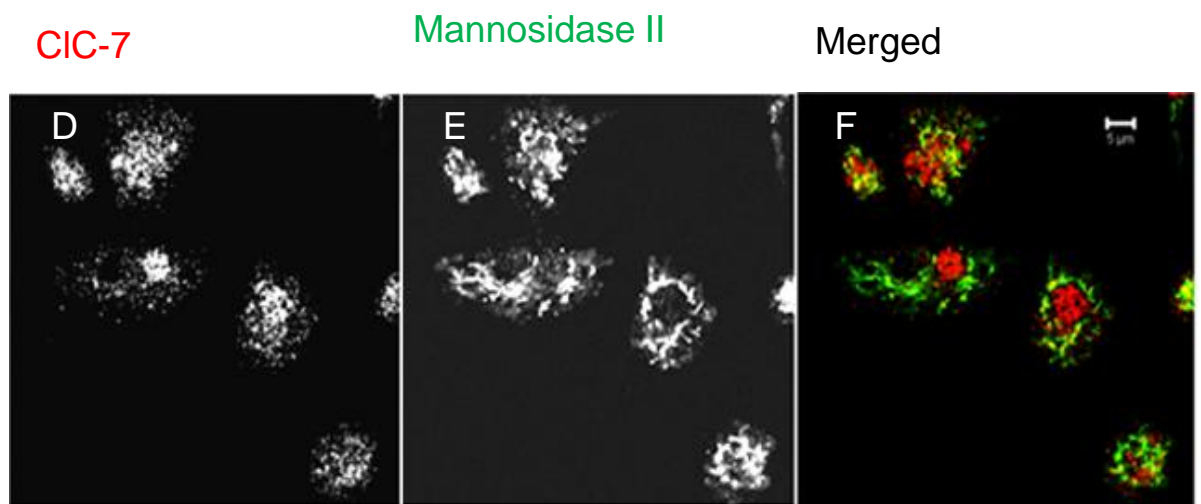
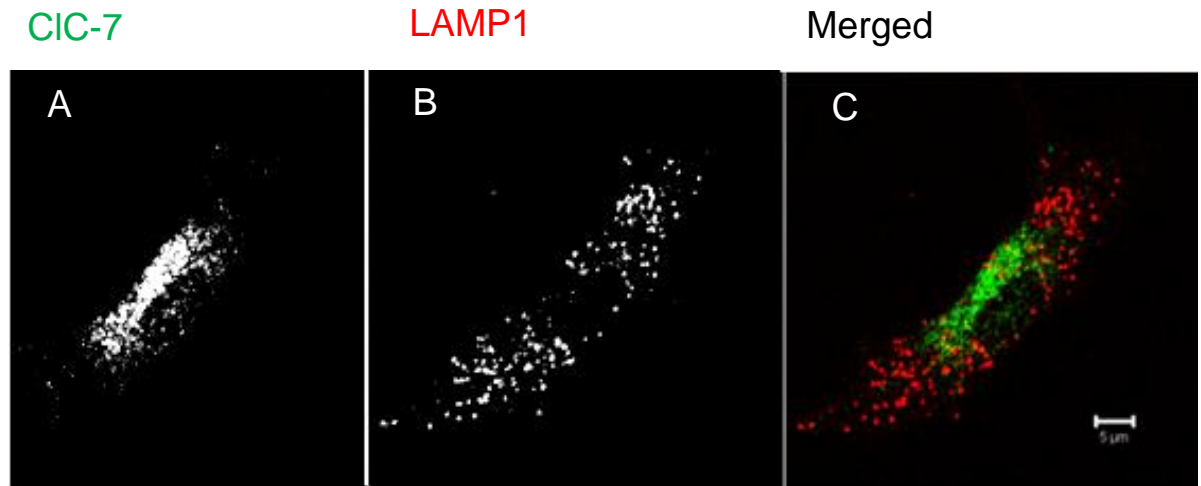
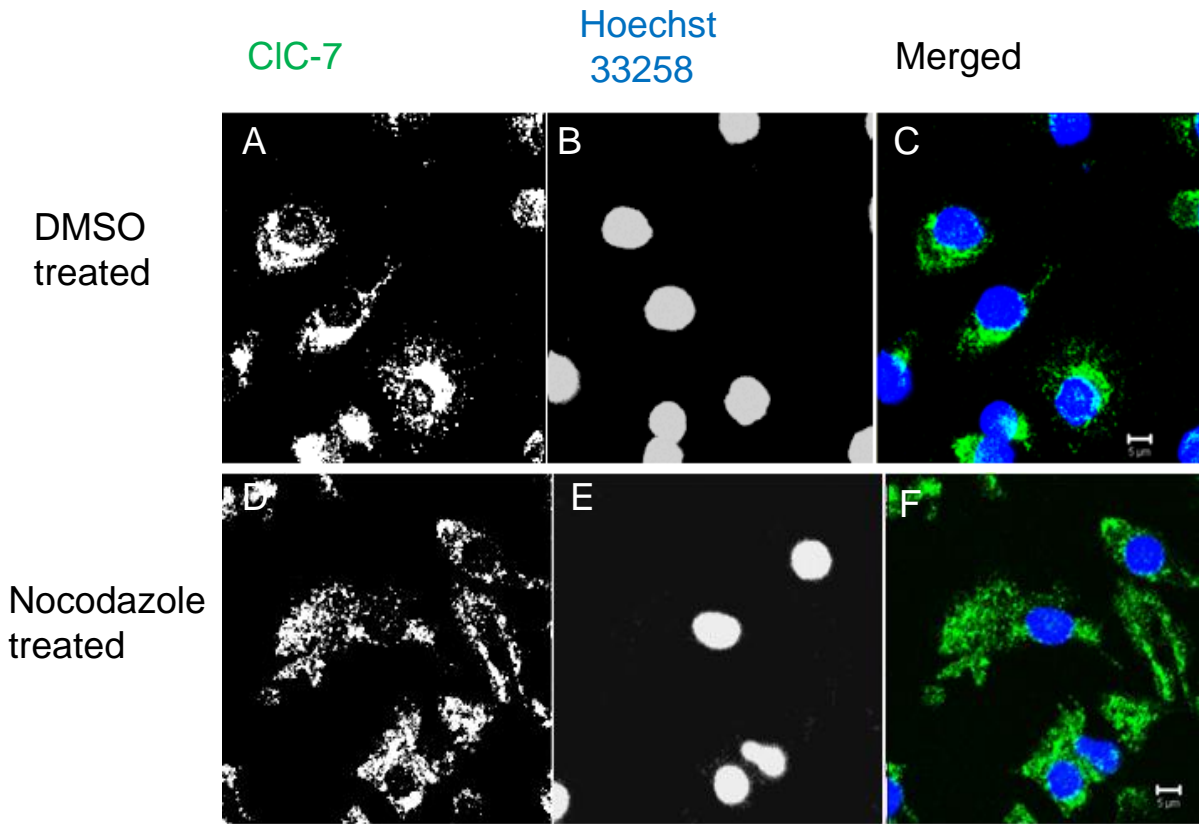
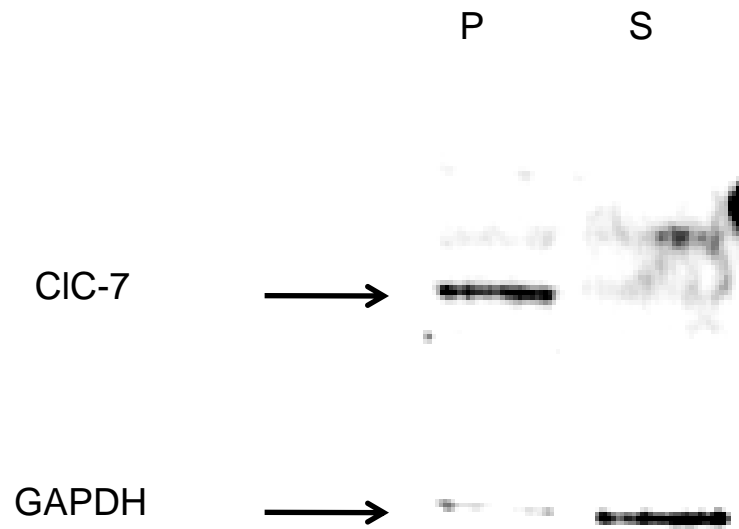




Figure S3



G. Detergent solubility of CIC-7 in microglia



**Figure S4**

CIC-7

Polyubiquitin

Merged

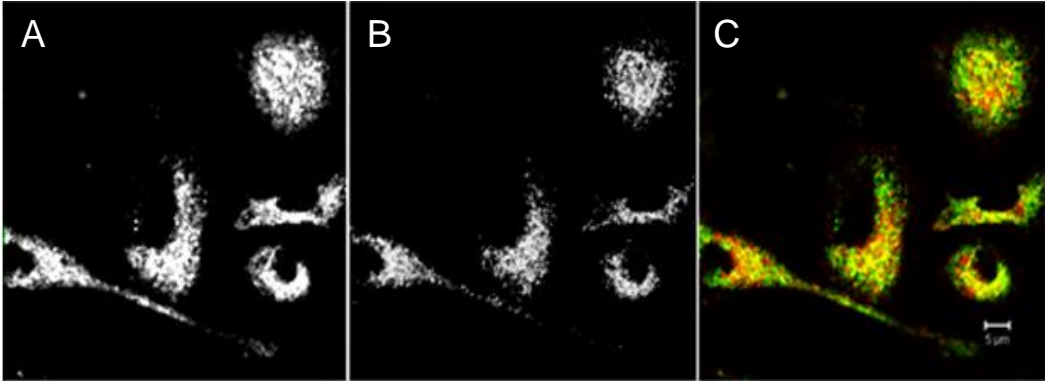


Figure S5

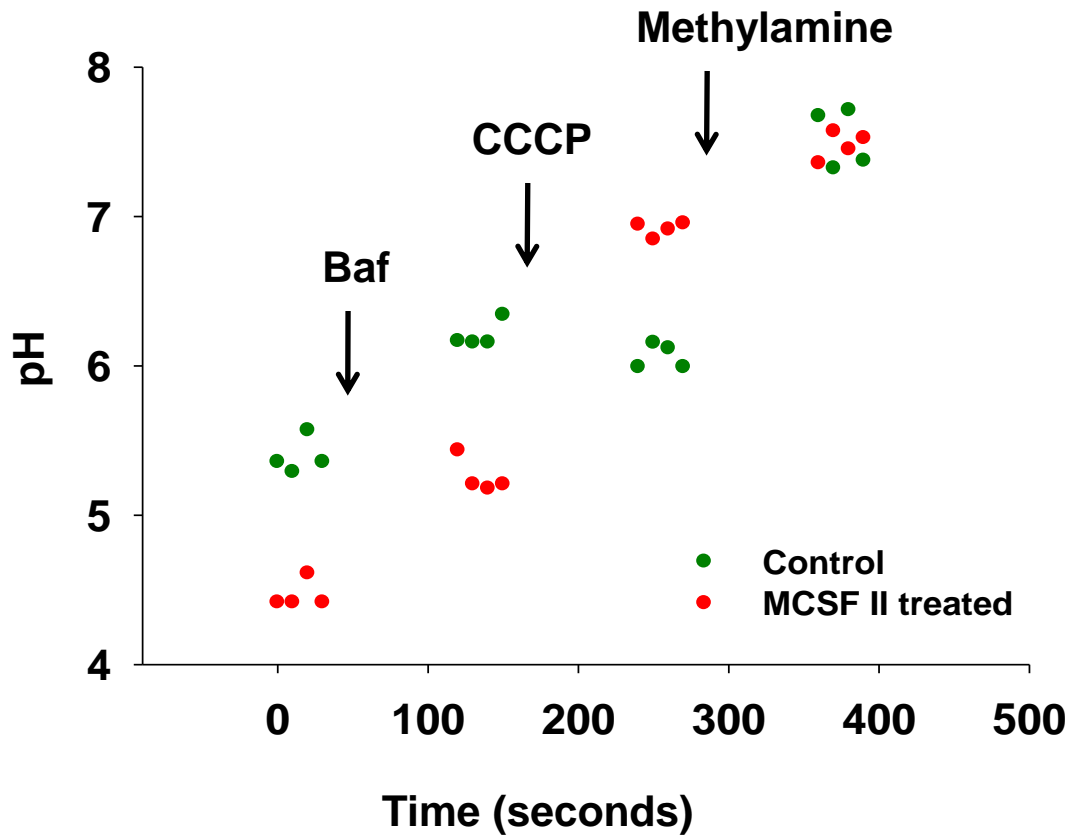
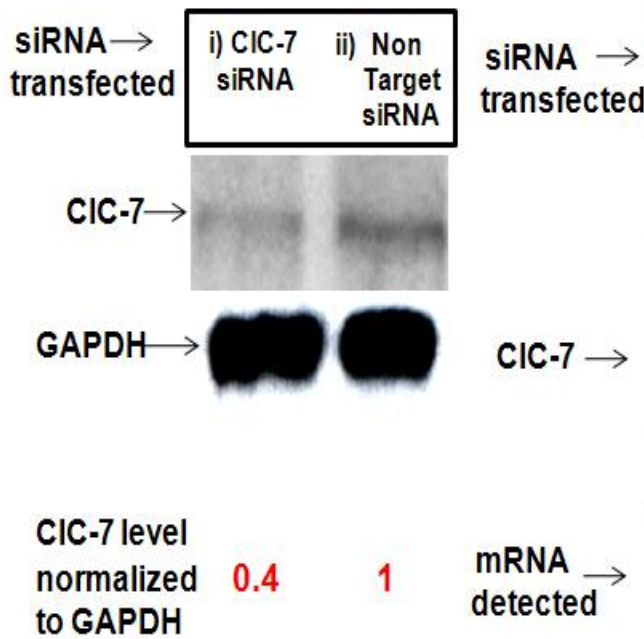
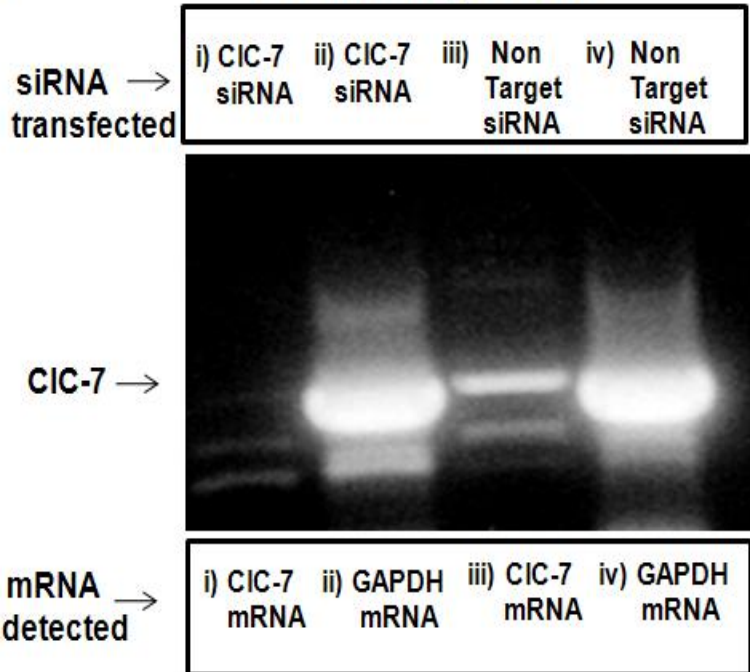


Figure S6

A) Knockdown of CIC-7 protein monitored by Western Blot.



B) Knockdown of CIC-7 mRNA monitored by RT-PCR



C) Knockdown of CIC-7 protein monitored by immunofluorescence.

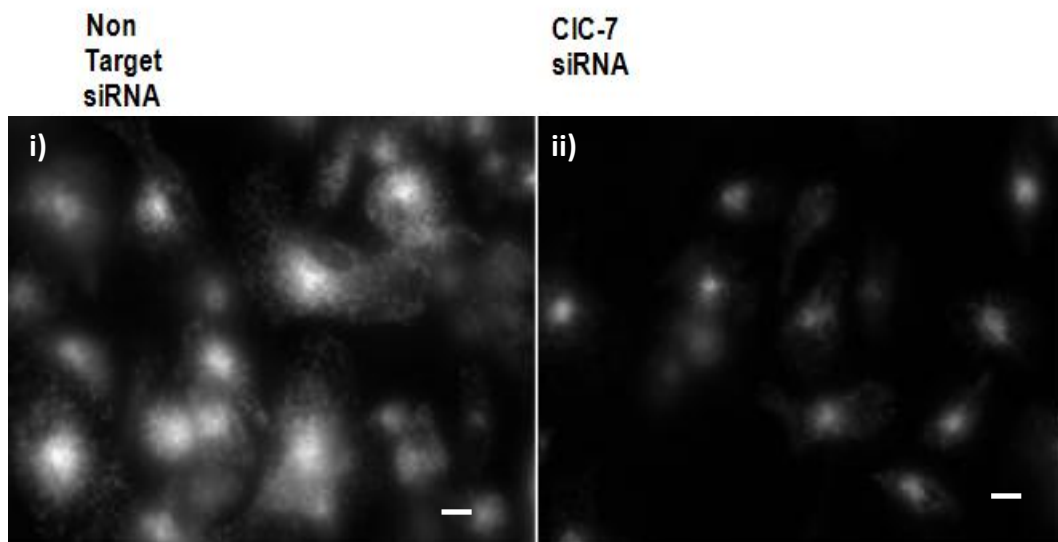
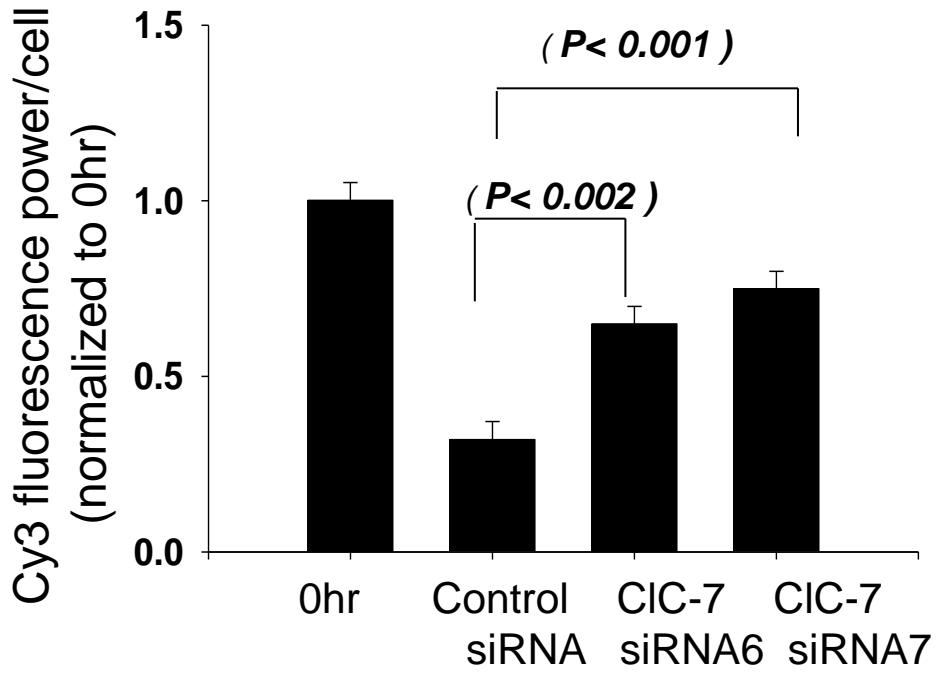
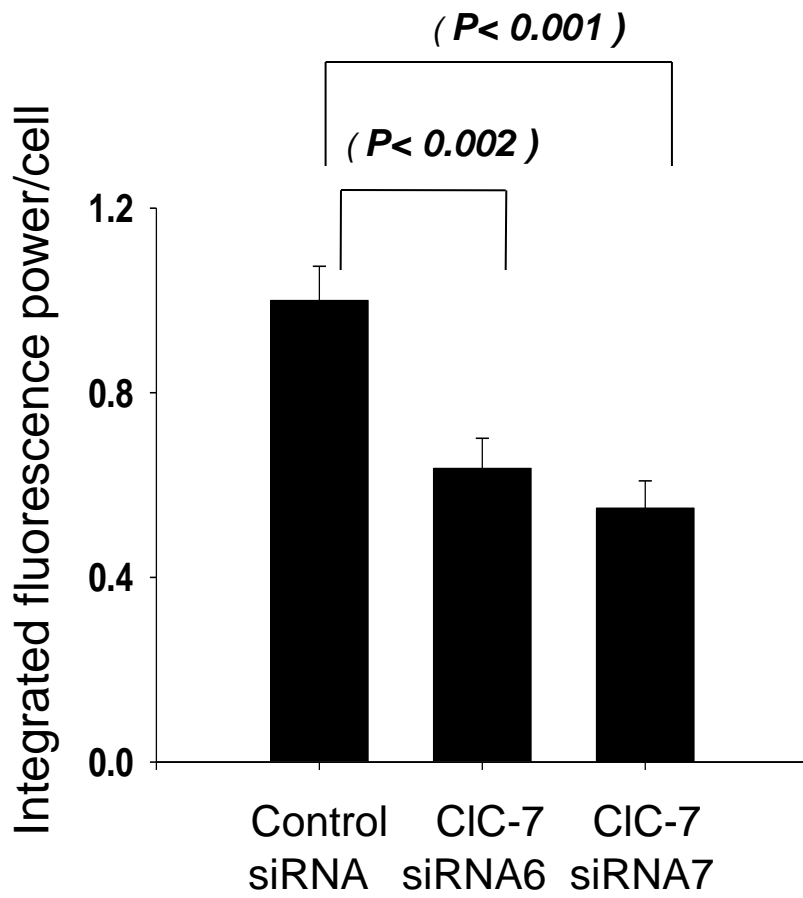


Figure S7

A

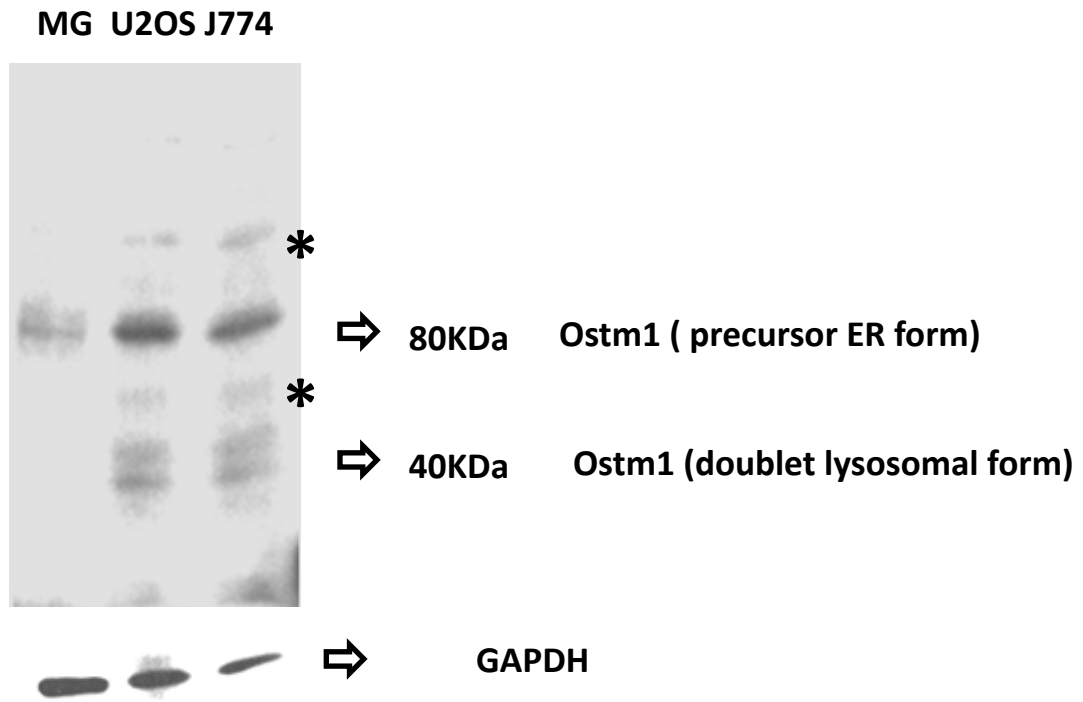


B



# Figure S8

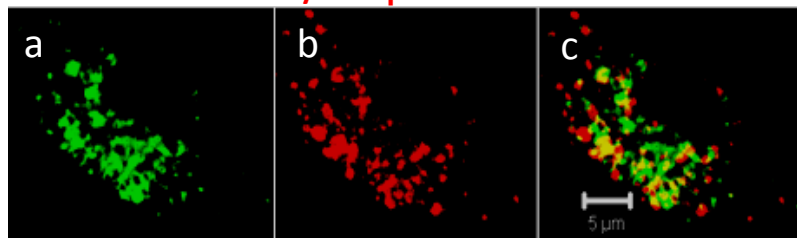
## A Expression of Ostm1 protein



## B CLC-7 max projection Mask-I Mask-II



## C V5-Ostm1 Cy3fA $\beta$ Merged



## D CLC-7 Ds-Red Merged

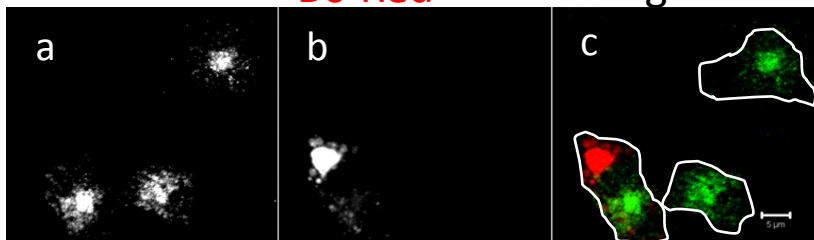
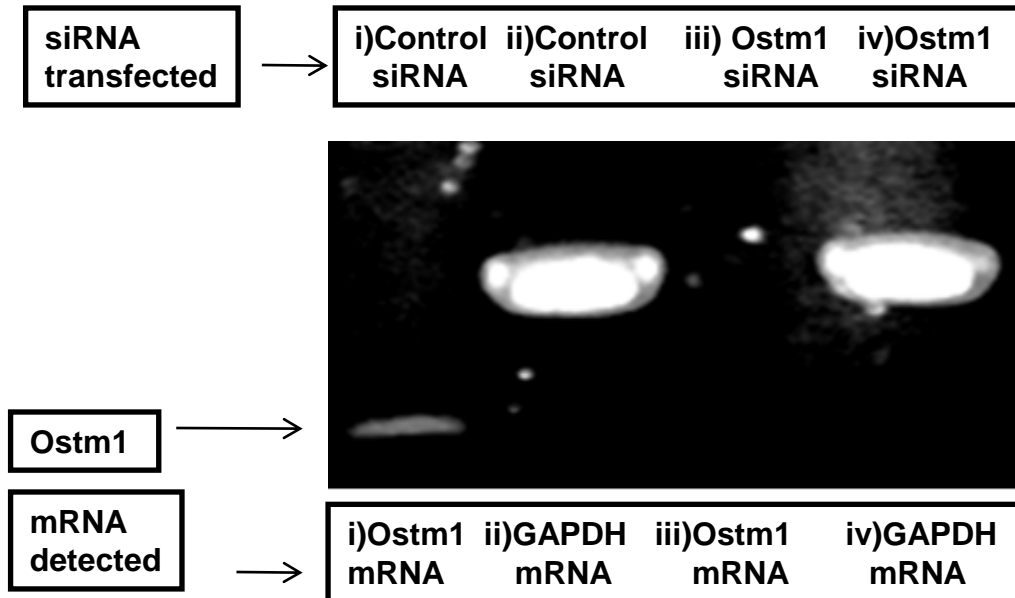


**Figure S9**

**A. Knockdown of Ostm1 mRNA monitored by RT-PCR**



**B. Knockdown of Ostm1 protein monitored by Western Blot**

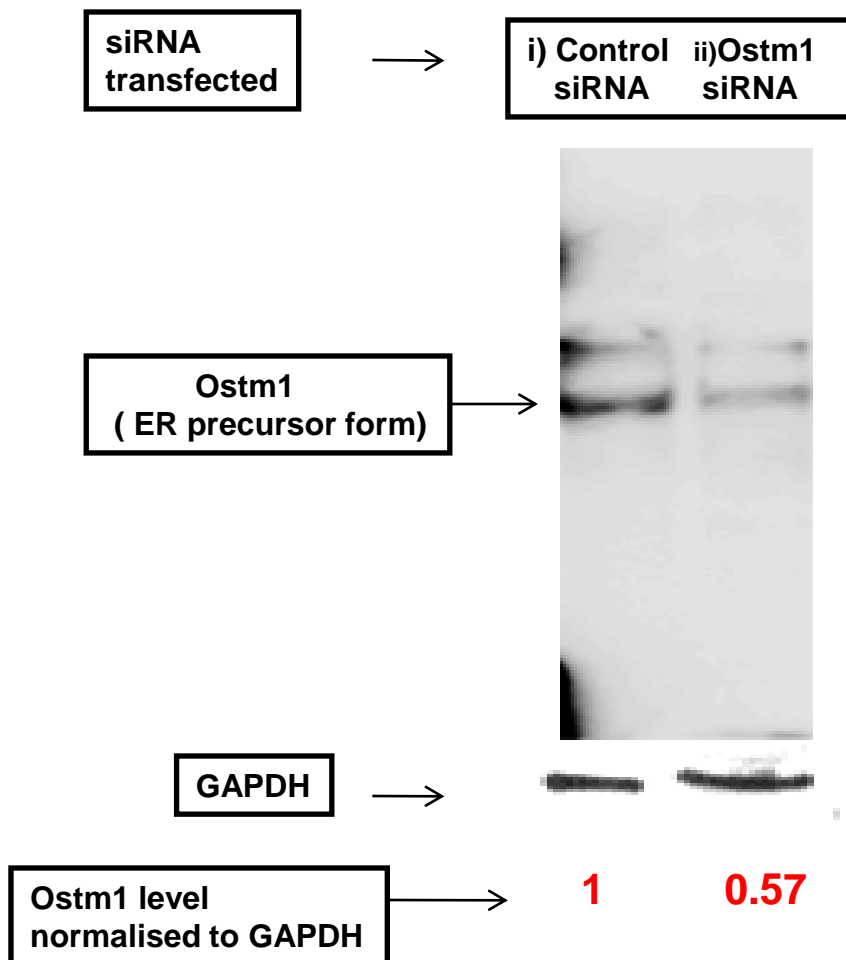


Figure S10

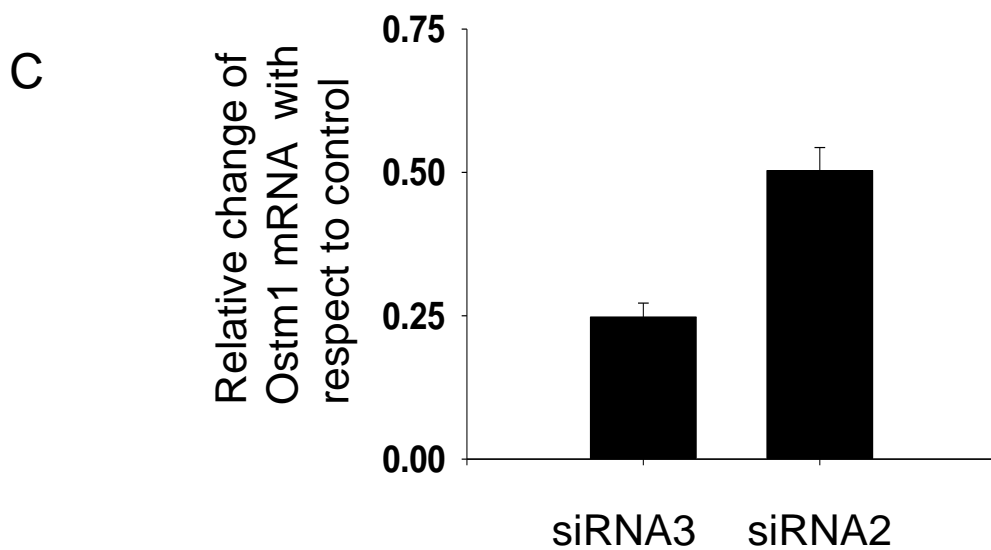
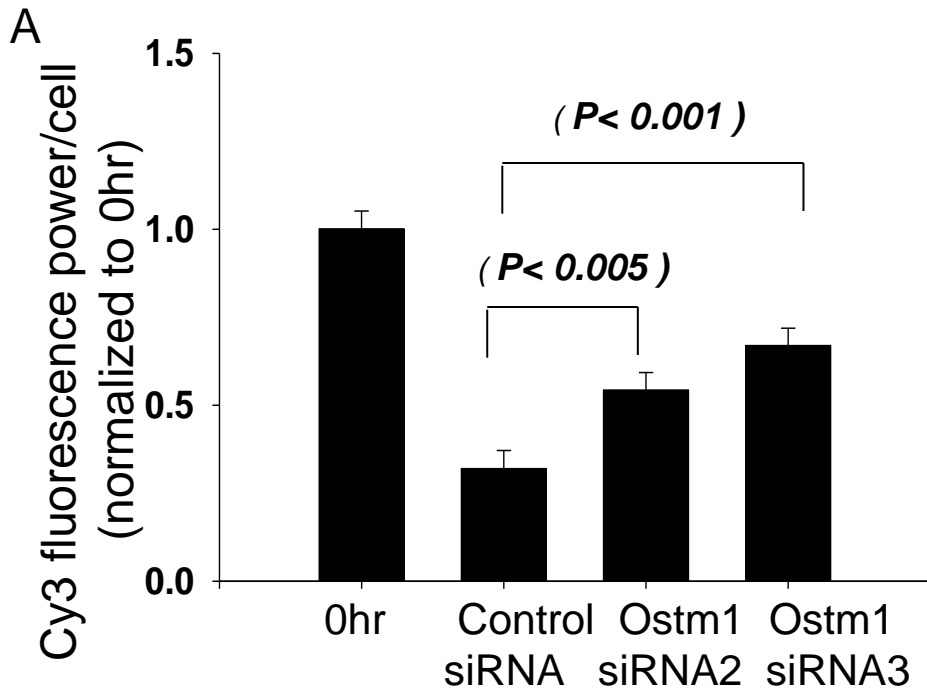




Figure S11

CIC-7

